DALTON
FULL PAPER

Ruthenium(II) complexes containing RuN_4O_2 spheres assembled *via* pyridine-imine-amide coordination. Syntheses, structures, properties and protonation behaviour of coordinated amide

Satyanarayan Pal and Samudranil Pal*

School of Chemistry, University of Hyderabad, Hyderabad 500 046, India

Received 28th November 2001, Accepted 19th February 2002
First published as an Advance Article on the web 27th March 2002

A series of ruthenium(II) complexes of general formula $[RuL_2]$ with the pyridine-N, the imine-N and the amide-O donor *N*-(aroyl)-*N*′-(picolinylidene)hydrazines (HL) has been synthesized. The ligands differ on the substituent at the *para* position of the aroyl fragment. The complexes have been characterized by analytical, ^{1}H NMR, electronic absorption spectroscopy and cyclic voltammetry. X-Ray structures of representative complexes have been determined. The lowest energy MLCT (Ru(dπ) ⟶ L(π*)) transitions for these complexes are observed at essentially identical wavelength (544 ± 1 nm). The complexes display a metal centred oxidation and a ligand centred reduction in the potential ranges 0.44 to 0.59 V and −1.49 to −1.35 V (*vs*. Ag/AgCl), respectively. The differences in the metal and ligand redox potentials ($\Delta E_{1/2}$) are practically same (1.94 ± 0.01 V) for all the complexes. The identical MLCT band positions and the same $\Delta E_{1/2}$ values suggest that in this series of complexes, the energy gap between the metal-dπ and the ligand-π* levels is constant. The effective pK_a values of the species obtained by protonation of the coordinated amide functionalities in one of the complexes have been evaluated by spectrophotometric titration. The corresponding diprotonated species has been characterized by X-ray crystallography.

Introduction

A vast literature on the ruthenium(II) complexes with α,α′-diimine ligands is now available.[1] Polypyridine ruthenium(II) complexes are most extensively studied and occupy the bulk of this literature. This is primarily due to their unique redox, photophysical and photochemical properties that are determined by the availability of low lying π* orbitals of the coordinated ligands and hence a low energy metal-to-ligand charge transfer excited state. These properties have led to increased utilisation of such ruthenium complexes in the studies on artificial photosynthesis,[2] photomolecular devices,[3] and protein and DNA structures and electron transfer in them.[4] Due to such wide range of applications there is a continuing quest for new ruthenium(II) complexes with different ligands containing the α,α′-diimine fragment[5,6] or with derivatives of polypyridine ligands.[7] The primary goal is to improve their efficiency in the above mentioned applications by modification of the coordinated ligands.

In the present work, we have studied the ruthenium(II) chemistry with tridentate *N*-(aroyl)-*N*′-(picolinylidene)hydrazines (HL, **I**). In deprotonated state, these Schiff bases can coordinate ruthenium(II) *via* the pyridine-N, the imine-N and the amide-O atoms and form neutral bis-chelates. The reasons for the choice of this ligand system are as follows. Like 2,2′-bipyridine they also contain the α,α′-diimine fragment which is π-acidic and can form a five-membered chelate ring with metal ions. The third coordinating centre, the O-atom of the deprotonated amide functionality is predominantly σ-basic which is opposite in character compared to the diimine fragment. The σ-basicity of this coordinating atom can be varied by using different substituents at the *para* position of the aroyl moiety. Thus the electron transfer properties of the complexes can be tuned by this variation. In addition to the above, this ligand system provides the scope of studying the effect of coordinated amide protonation state on the physical properties of the complex. Herein, we describe the synthesis and characterization of a new series of ruthenium(II) complexes with the above ligand system. X-Ray structures of representative complexes have been determined. In solution, electron transfer and spectral properties, and protonation behavior of the coordinated amide have been investigated.

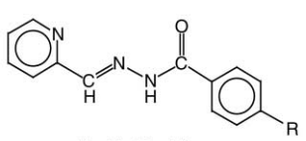

Hpabh (R = H)
Hpach (R = Cl)
Hpath (R = Me)
Hpamh (R = OMe)
Hpadh (R = NMe_2)

(I)

Results and discussion

Synthesis and some properties

The dark brown complexes were synthesized in good yields by reacting $[Ru(dmso)_4Cl_2]$, HL and NaOH in 1 : 2 : 2 mole ratio in boiling methanol. In each case, the complex was precipitated from the reaction mixture. However chromatographic purification was necessary on a neutral aluminium oxide column. Elemental analysis data (Table 1) are satisfactory with the molecular formula $[RuL_2]$ (L^- = $pach^-$, $pabh^-$, $path^-$, $pamh^-$ and $padh^-$). All the complexes are electrically non-conducting in CH_3CN solutions. They are diamagnetic and NMR active. Thus the metal ions in these complexes are in +2 oxidation state and low-spin in character.

Structures of $[Ru(pabh)_2]$ 2 and $[Ru(path)_2]$ 3

The molecular structures of **2** and **3** are illustrated in Figs. 1 and 2, respectively. The selected bond parameters associated with the metal ions are listed in Table 2. In each complex, the metal ion is in distorted octahedral N_4O_2 coordination sphere

 DOI: 10.1039/b110912j

Table 1 Elemental analysis[a] and electronic absorption spectral[b] data

Complex	Microanalysis (%) C	H	N	λ_{max}/nm (ε/dm^3 mol^{-1} cm^{-1})
1 [Ru(pach)$_2$]	50.13 (50.49)	2.84 (2.93)	13.31 (13.59)	545 (9790), 487[c] (5063), 433[c] (3440), 396[c] (16890), 373[c] (27950), 337 (47070), 257 (28560)
2 [Ru(pabh)$_2$]	56.70 (56.82)	3.74 (3.67)	15.14 (15.29)	544 (11410), 486[c] (5020), 431[c] (3590), 394[c] (17585), 370[c] (28467), 335 (43253), 251 (27269)
3 [Ru(path)$_2$]	58.06 (58.22)	4.31 (4.19)	14.39 (14.55)	544 (11474), 489[c] (5853), 433[c] (3966), 395[c] (23603), 371[c] (36694), 340 (50440), 256 (28012)
4 [Ru(pamh)$_2$]	54.95 (55.17)	3.86 (3.97)	13.64 (13.79)	543 (15713), 486[c] (7892), 437[c] (5388), 396[c] (41964), 373[c] (62810), 348 (71965), 272[c] (29968), 246 (35144)
5[Ru(padh)$_2$]	56.41 (56.68)	4.69 (4.76)	17.50 (17.62)	545 (9791), 492[c] (6447), 407 (61402), 282 (27262)

[a] Required values are given in parentheses. [b] In CH_3CN solutions. [c] Shoulder.

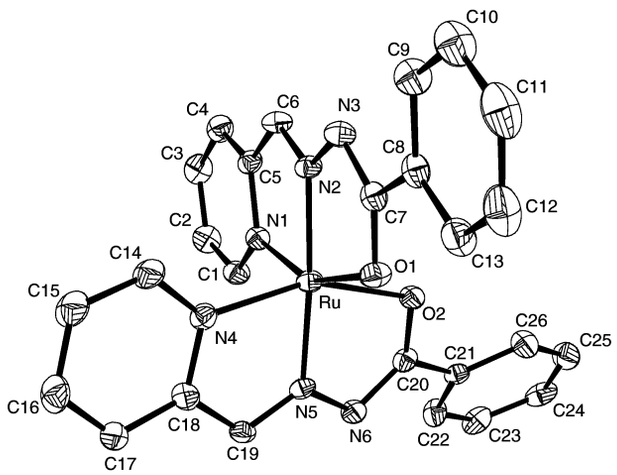

Fig. 1 Structure of [Ru(pabh)$_2$] **2** with the atom-labeling scheme. All atoms are represented by their 25% probability thermal ellipsoids. Hydrogen atoms are omitted for clarity.

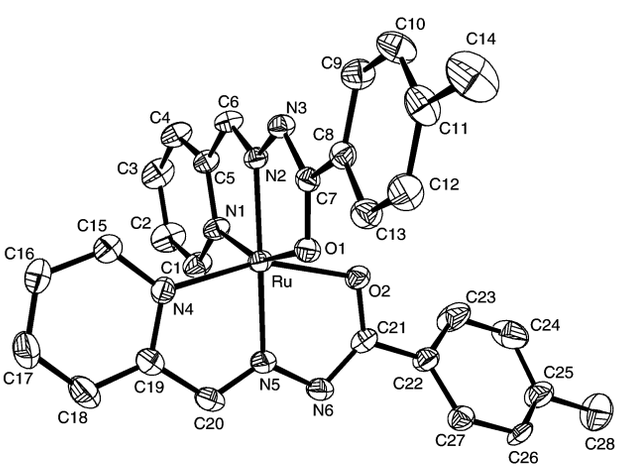

Fig. 2 Structure of [Ru(path)$_2$] **3** showing 25% probability thermal ellipsoids and the atom-labeling scheme. For clarity, hydrogen atoms are omitted and only one of the two orientations of the disordered tolyl ring (C22–C27) is shown.

assembled *via* the meridionally spanning pyridine-N, imine-N and deprotonated amide-O donor tridentate ligands. The N–N, N–C and C–O distances in the =N–N=C(O$^-$) fragments of the coordinated ligands in both complexes are in the range 1.374(6)–1.384(4) Å, 1.310(7)–1.323(5) Å and 1.281(6)–1.292(4) Å, respectively. These distances are consistent with the enolate form of the amide functionalities in each complex.[8] In both complexes, the average chelate bite angles in the five-membered rings formed by the pyridine-N and the imine-N are slightly larger than that in the five-membered rings formed by the amide-O and the imine-N. The former values are 79.03 and 79.25° and the latter 76.44 and 76.5° for [Ru(pabh)$_2$] and [Ru(path)$_2$], respectively. The Ru(II)–N(pyridine) bond lengths are within the range reported for Ru(II) complexes having the same coordinating atom.[7,9] The Ru(II)–N(imine) bond lengths are comparable with those reported earlier.[6] However the Ru(II)–N(pyridine) bond lengths (2.010(5)–2.042(3) Å) are significantly longer than the Ru(II)–N(imine) bond lengths (1.957(5)–1.962(4) Å). Most probably this difference is mainly due to the rigidity of the tridentate ligand.[10] Better π-back-bonding in the Ru(II)–N(imine) bond compared to that in the Ru(II)–N(pyridine) bond[11] may also be partially responsible for this difference. The Ru(II)–O(amide) bond lengths in [Ru(pabh)$_2$] are longer than those in [Ru(path)$_2$]. This is most likely due to better Ru(II)–O σ-bonding in the latter compared to that in the former. This difference in the σ-bond strength can be rationalized considering the presence of electron releasing methyl group at the *para* position of the aroyl fragment in path$^-$.

Table 2 Selected bond distances (Å) and angles (°) with their standard deviations for [Ru(pabh)$_2$] **2** and [Ru(path)$_2$] **3**

	2	**3**
Ru–N(1)	2.037(3)	2.047(5)
Ru–N(2)	1.960(3)	1.962(4)
Ru–N(4)	2.042(3)	2.010(5)
Ru–N(5)	1.958(3)	1.957(5)
Ru–O(1)	2.137(3)	2.106(4)
Ru–O(2)	2.115(3)	2.108(4)
N(1)–Ru–N(2)	79.03(13)	79.11(19)
N(1)–Ru–N(4)	97.09(13)	90.4(2)
N(1)–Ru–N(5)	96.08(13)	101.3(2)
N(1)–Ru–O(1)	155.01(11)	155.90(17)
N(1)–Ru–O(2)	89.99(11)	95.17(18)
N(2)–Ru–N(4)	99.31(13)	99.75(19)
N(2)–Ru–N(5)	174.65(13)	179.1(2)
N(2)–Ru–O(1)	76.09(12)	76.79(17)
N(2)–Ru–O(2)	105.18(11)	104.65(17)
N(4)–Ru–N(5)	79.03(13)	79.4(2)
N(4)–Ru–O(1)	89.17(12)	93.09(17)
N(4)–Ru–O(2)	155.39(11)	155.58(17)
N(5)–Ru–O(1)	108.87(11)	102.8(2)
N(5)–Ru–O(2)	76.80(12)	76.20(18)
O(1)–Ru–O(2)	94.29(10)	91.41(15)

Spectral characteristics

In the infrared spectrum, none of the complexes displays the characteristic bands associated with the N–H and C=O bonds of the amide functionality[12] present in the free Schiff bases. Thus in the complex the amide functionality is deprotonated and exists in the enolate form. A medium to strong band observed in the range 1593–1605 cm^{-1} is possibly due to the conjugate C=N–N=C fragment[13] of the coordinated ligand.

Table 3 Cyclic voltammetric data[a]

Complex	Metal-centred oxidation $E_{1/2}$/V (ΔE_p/mV)	Ligand-based reduction $E_{1/2}$/V (ΔE_p/mV)
1 [Ru(pach)$_2$]	0.59 (70)	−1.35 (70)
2 [Ru(pabh)$_2$]	0.56 (70)	−1.38 (70)
3 [Ru(path)$_2$]	0.54 (70)	−1.40 (80)
4 [Ru(pamh)$_2$]	0.52 (80)	−1.42 (70)
5 [Ru(padh)$_2$]	0.44 (70)	−1.49 (70)

[a] $E_{1/2} = (E_{pa} + E_{pc})/2$, where E_{pa} and E_{pc} are anodic and cathodic peak potentials, respectively; $\Delta E_p = E_{pa} - E_{pc}$; scan rate, 100 mV s^{-1}.

The proton NMR spectra of all the five complexes clearly suggest that in solutions both ligands in each complex are magnetically equivalent. The aromatic protons resonate in the range δ 6.58–8.13. The azomethine hydrogen appears as a singlet in the range δ 8.75–8.89. An interesting observation is that as the electron donating ability of the substituent on the aroyl moiety of the ligand increases the signal corresponding to the azomethine proton displays a high-field shift. For the three complexes, [Ru(path)$_2$], [Ru(pamh)$_2$] and [Ru(padh)$_2$], the methyl protons of the substituent on the aroyl fragment of the ligands are observed as singlets at δ 2.36, 3.81 and 2.98, respectively.

The electronic absorption spectral data for the complexes are collected in Table 1. The spectral profiles are very similar. All the complexes display the lowest energy band at 544 ± 1 nm with absorption coefficients in the order of 10^4 dm^3 mol^{-1} cm^{-1}. In each case, a shoulder in the range 486–492 nm follows this band. These bands are assigned to metal-to-ligand (Ru(dπ) ⟶ L(π*)) charge transfer transitions (MLCT). Broad mutiple MLCT bands for this type of complexes are not unusual considering the possibility of several acceptor levels of different energies being available.[5,14] This spectral profile in the visible region is strikingly similar to those of tris(diimino) complexes of ruthenium(II) ([RuL$_3$]$^{2+}$ where L is 2,2′-bipyridine or aryl-(2-pyridylmethylene)amine).[5] It is interesting to note that the present series of complexes display the lowest energy MLCT band at a much longer wavelength compared to that displayed by the above mentioned [RuL$_3$]$^{2+}$ species (454 nm when L = 2,2′-bipyridine and 480 nm when L = aryl(2-pyridylmethylene)-amine). At higher energy the complexes display two very intense bands in the range 335–407 nm and 251–282 nm. The former is preceded by several shoulders (Table 1). The first intense absorption shows a high-energy shift as the substituent on the aroyl moiety becomes more electron withdrawing. The main spectral features for the complexes in the higher energy range are very similar with those of the corresponding free Schiff bases. In general for each complex these bands are at longer wavelengths compared to the band positions displayed by the corresponding free Schiff base. The Schiff bases display a weak band (ε 396–1222 dm^3 mol^{-1} cm^{-1}) in the range 375–412 nm followed by two intense peaks in the range 299–335 and 211–245 nm. The first two absorptions display a high-energy shift with the increasing electron withdrawing nature of the substituent on the aroyl moiety. Thus except the two lowest energy absorptions the other higher energy absorptions observed for the complexes are assigned to the intraligand transitions.

Redox properties

Electron transfer properties of all the complexes have been studied by cyclic voltammetry in acetonitrile solutions (0.1 M TBAP). The potential data are listed in Table 3 and representative cyclic voltammograms are illustrated in Fig. 3. Each complex displays a metal centred oxidation response and a ligand centred reduction response on the anodic and cathodic side of the Ag/AgCl electrode, respectively. The one electron stoichiometry of these responses is established by coulometry.

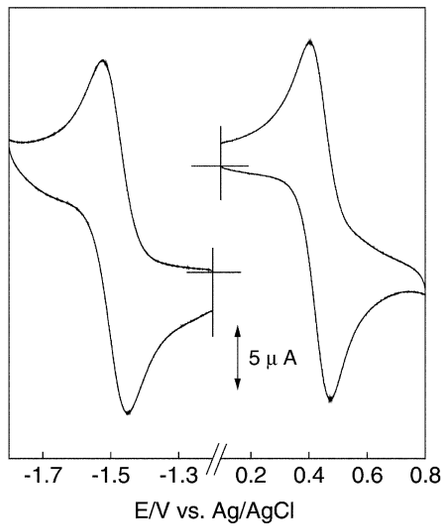

Fig. 3 Cyclic voltammograms (scan rate 100 mV s^{-1}) of [Ru(padh)$_2$] **5** in acetonitrile (0.1 mol dm^{-3} TBAP) at a glassy carbon working electrode at 298 K.

The oxidation response is assigned to couple (1) and the reduction response is assigned to couple (2). The potentials for both couples are sensitive to the polar effect of the substituent on the aroyl moiety of the ligand. For each couple the potential gradually decreases as the substituent becomes

$$[Ru^{III}L_2]^+ + e^- \rightleftharpoons [Ru^{II}L_2] \quad (1)$$

$$[Ru^{II}L_2] + e^- \rightleftharpoons [Ru^{II}L(L^{\bullet})]^- \quad (2)$$

more and more electron releasing. Plots of $E_{1/2}$ against the Hammett substituent constant (σ_p)[15] are satisfactorily linear. The effect of substituent on the potential ($E_{1/2}$(Ru)) of couple (1) and on that ($E_{1/2}$(L)) of couple (2) is the same within experimental error (Table 3). As a consequence the value of $\Delta E_{1/2}$ ($E_{1/2}$(Ru) − $E_{1/2}$(L)) is essentially identical (1.94 ± 0.01 V) for all the complexes (Table 3). In additon, $E_{1/2}$(Ru) is linearly correlated with $E_{1/2}$(L) (Fig. 4) with a slope very close to unity

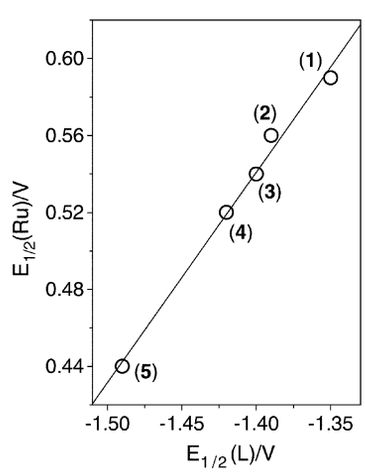

Fig. 4 Correlation between $E_{1/2}$(Ru) and $E_{1/2}$(L) values. The straight line represents a linear least-squares fit.

(1.09(6)). A possible rationale for these observations is as follows. An electron withdrawing group on the aroyl fragment of the ligand decreases π-donor capability of the O-atom of the deprotonated amide functionality and hence increases the effective nuclear charge on the ruthenium centre. As a result the energy of the metal-dπ orbitals and that of the ligand-π*

orbitals are lowered.[16] The ensuing metal-dπ to ligand-π* back-bonding further stabilizes the metal-dπ orbitals however destabilizes the ligand-π* orbitals. The $\Delta E_{1/2}$ values and the slope of the straight line obtained by plotting $E_{1/2}$(Ru) against $E_{1/2}$(L) reflect the extent of changes in the metal-dπ and the ligand-π* levels.[17] In the present series of complexes, the very similar values of $\Delta E_{1/2}$ and a slope very close to unity suggest that the net perturbations in the metal-dπ and the ligand-π* levels are the same due to the polar effect of the substituent on the aroyl fragment of the ligand. This is also substantiated by essentially identical lowest energy band positions (544 ± 1 nm) observed in the electronic spectra of these complexes (*vide supra*) due to MLCT transitions that involve excitation of electron from metal-dπ to ligand-π* level.

Protonation behaviour of [Ru(pabh)$_2$] 2

Protonation behaviour of the coordinated amide functionalities in **2** has been studied by spectrophotometric titration using acetonitrile solutions of the complex and CF_3SO_3H. With the progressive addition of the acid the absorptions are blue-shifted (Fig. 5). The interesting aspect of the titration is that the extent

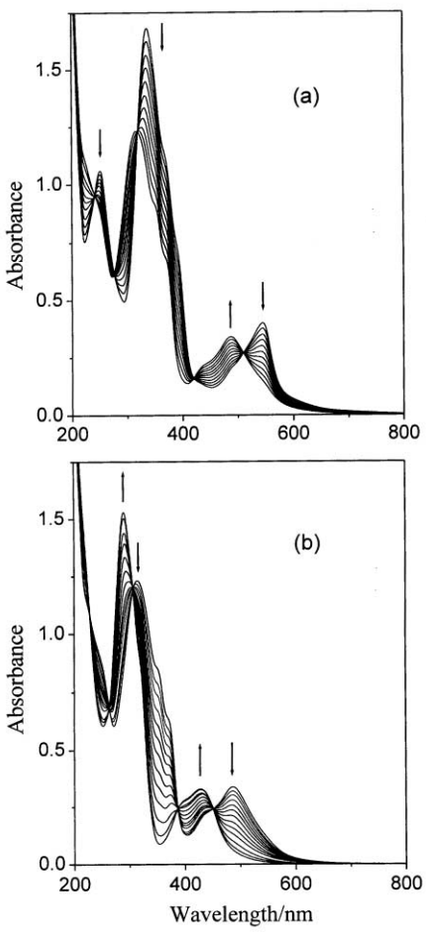

Fig. 5 Spectrophotometric titration of [Ru(pabh)$_2$] **2** in acetonitrile with CF_3SO_3H. (a) First segment of the titration. (b) Second segment of the titration (see text).

of change in the spectral profile gradually decreases and when the complex to acid mole ratio becomes about 1 : 1.1 it becomes a minimum. Fig. 5(a) depicts the shift of band positions through five isosbestic points in this region of the titration. These isosbestic points are at 509, 421, 319, 276, and 241 nm. However continued addition of the acid causes a further shift of band positions to higher energy through a different set of five isosbestic points (at 451, 387, 307, 263, and 228 nm) and at about 1 : 2.4 complex to acid mole ratio the spectral profile becomes constant (Fig. 5(b)). The observation of two sets of isosbestic points clearly suggest two sequential protonation of the pair of metal coordinated amide functionalities present in the complex. Quantitative reversibility of this protonation behavior was confirmed by spectrophotometric back-titration with $(C_2H_5)_3N$. The effective pK_{ai} (i = 1 and 2) values were determined from the two segments (Fig. 5(a) for pK_{a2} and Fig. 5(b) for pK_{a1}) of the spectrophotometric titration using eqns. (3), (4) and (5).[18] The value of $K_a(CF_3SO_3H)$ in

$$K_{ai} = K_a(CF_3SO_3H)/K_{ci} \quad (3)$$

$$K_{c1} = [\text{complex}H_2^{2+}][CF_3SO_3^-]/[\text{complex}H^+][CF_3SO_3H] \quad (4)$$

$$K_{c2} = [\text{complex}H^+][CF_3SO_3^-]/[\text{complex}][CF_3SO_3H] \quad (5)$$

acetonitrile was obtained from ref. 19. The change in absorbance at 486.5 nm and that at 544 nm were used to calculate K_{c1} and K_{c2}, respectively. The values of pK_{a1} and pK_{a2} thus obtained are 6.85(5) and 7.44(9), respectively. The large pK value (~15)[20] of free amide functionality in organic compounds suggest that the –C(=O)NH– proton is very weakly acidic. It is interesting that although in the diprotonated species (complexH_2^{2+}), and possibly in the monoprotonated species (complexH^+), the amide functionalities are not bound to the metal ion (*vide infra*) still the acidity of the amide proton increases by ~8 orders of magnitude. A possible rationale could be as follows. The electron deficiency of the N-atom adjacent to the protonated amide N-atom arising out of the coordination of the former to the Ru(II) centre is partially compensated by the free amide moiety. As a consequence the N-centre in the amide functionality becomes less basic and hence the attached proton becomes more acidic. In some ruthenium(II) complexes with Schiff bases derived from phenylhydrazine and 2-hydroxyaldehydes, a similar increase in acidity of the N–H proton due to metal coordination to the adjacent N-atom has been noted.[21]

Isolation and characterization of the diprotonated complex

We are unable to grow X-ray quality crystals of $CF_3SO_3^-$ salts of the monoprotonated and diprotonated species. However slow evaportaion of an acetonitrile solution of [Ru(pabh)$_2$] and $HClO_4$ (1 : 2.5 mole ratio) produces a light brown crystalline material. X-Ray structure determination (*vide infra*) of this material reveals the protonation of both amide functionalities in [Ru(pabh)$_2$]. This diprotonated complex crystallizes as [Ru(Hpabh)$_2$(CH$_3$CN)$_2$](ClO$_4$)$_2$·H$_2$O **6**. A similar approach to obtain the crystals of the ClO_4^- salt of the monoprotonated species failed. The diprotonated complex **6** starts loosing solvent immediately after isolation and becomes a light brown amorphous solid. The exact nature of this amorphous solid is not clear at present. The infrared spectrum does not indicate the presence of the acetonitrile molecules. The perchlorate ions display a strong and broad peak at ~1100 cm^{-1} and a sharp peak at ~620 cm^{-1}. A broad peak centred at ~3440 cm^{-1} and a sharp peak at 2924 cm^{-1} are likely to be associated with the water molecule and amide N–H stretches, respectively. The strong peak observed at 1682 cm^{-1} is possibly due to the amide C=O moiety.

Because of the solvent loss problem the solution properties of the crystalline complex were studied by dissolving it in acetonitrile within 5 min after isolation of the crystals and the concentration was calculated assuming the molecular formula [Ru(Hpabh)$_2$(CH$_3$CN)$_2$](ClO$_4$)$_2$·H$_2$O **6**, as found in the X-ray structure determination. In acetonitrile, the complex behaves as a 1 : 2 electrolyte. The molar conductivity value is 263 Ω^{-1} cm^2 mol^{-1}. The electronic spectrum in acetonitrile solution displays a peak at 429 nm (ε = 7500 dm^3 mol^{-1} cm^{-1}) followed by two shoulders (393 and 323 nm) and another peak at 290 nm

Table 4 Selected bond distances (Å) and angles (°) with their standard deviations for $[Ru(Hpabh)_2(CH_3CN)_2](ClO_4)_2 \cdot H_2O$ **6**

Ru–N(1)	2.036(6)	Ru–N(2)	2.050(6)
Ru–N(4)	2.059(6)	Ru–N(5)	2.055(6)
Ru–N(7)	2.042(7)	Ru–N(8)	2.042(7)
N(1)–Ru–N(2)	78.0(2)	N(1)–Ru–N(4)	88.7(2)
N(1)–Ru–N(5)	96.0(2)	N(1)–Ru–N(7)	91.8(3)
N(1)–Ru–N(8)	172.3(2)	N(2)–Ru–N(4)	94.7(3)
N(2)–Ru–N(5)	170.8(2)	N(2)–Ru–N(7)	91.8(3)
N(2)–Ru–N(8)	94.4(3)	N(4)–Ru–N(5)	78.0(2)
N(4)–Ru–N(7)	173.5(3)	N(4)–Ru–N(8)	93.0(2)
N(5)–Ru–N(7)	95.5(3)	N(5)–Ru–N(8)	91.7(3)
N(7)–Ru–N(8)	87.4(3)		

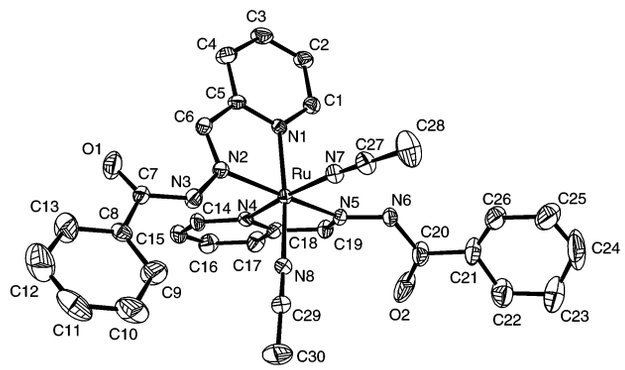

Fig. 6 Structure of the cation in $[Ru(Hpabh)_2(CH_3CN)_2](ClO_4)_2 \cdot H_2O$ **6** showing 20% probability thermal ellipsoids and the atom-labeling scheme. Hydrogen atoms are omitted for clarity.

(ε = 34 200 dm^3 mol^{-1} cm^{-1}). This spectral profile is identical with that obtained from a mixture of $[Ru(pabh)_2]$ **2** and CF_3SO_3H (1 : 2.8 mole ratio) in acetonitrile (Fig. 5(b)). The ^{1}H NMR spectrum in CD_3CN displays the N–H proton at δ 10.53 and the =C–H proton at δ 9.69. The aromatic protons are observed in the range δ 7.62–8.04. Thus in solution both the Hpabh ligands of **6** are magnetically equivalent.

The structure of the complex cation in **6** is illustrated in Fig. 6. The selected bond parameters associated with the Ru(II) centre are given in Table 4. The metal centre in **6** is in distorted octahedral N_6 coordination sphere. Each of the two Hpabh ligands act as bidentate ligand and coordinates the metal ion through the pyridine-N and the imine-N atoms forming a five-membered chelate ring. Two acetonitrile-N atoms occupy the remaining two mutually *cis* coordination sites. The N–N, N–C and C–O bond lengths in the =N–NH–C(=O) fragments of the two coordinated ligands are 1.386(8), 1.375(8); 1.340(10), 1.363(10); and 1.191(11), 1.226(12), respectively. Comparison of these bond lengths with the corresponding bond lengths in **2** clearly indicate that the amide fragments in **6** are protonated. Thus when the amide functionalities in **2** are protonated the Ru(II)–O(amide) bonds are dissociated and the N-atoms of two acetonitrile molecules coordinate the metal ion at the same two sites. The Ru(II)–N(pyridine) bond lengths (2.036(6) and 2.059(6) Å) are essentially identical with those in **2**. However the Ru(II)–N(imine) distances (2.050(6) and 2.055(6) Å) are significantly longer than those (1.960(3) and 1.958(3) Å) in **2**. As mentioned above, the rigidity of the pabh$^-$ ligands in **2** arising from its tridentate binding mode and the fact that the imine-N is the middle coordinating atom are likely to be the reasons for the shorter Ru(II)–N(imine) bond lengths in **2** compared to those in **6**. The Ru(II)–N(acetonitrile) bond lengths are unexceptional.[22]

Conclusion

A new series of mononuclear ruthenium(II) complexes with the N,N,O-donor *N*-(aroyl)-*N′*-(picolinylidene)hydrazines has been described. It has been demonstrated that the polar effect of the substituent on the ligand affects the energies of the metal-dπ and the ligand-π* levels, however, the energy difference between them remains constant in all the complexes. The coordinated amide functionalities can be reversibly protonated and deprotonated. The X-ray structure reveals that in the diprotonated species the ligands act as bidenate N,N-donor and the ruthenium(II) centre prefers two acetonitrile-N atoms instead of the O atoms of the protonated amide functionalities in the coordination sphere.

Experimental

Materials

$[Ru(dmso)_4Cl_2]$ was prepared by following a reported procedure.[23] The Schiff bases were obtained in 80–90% yield by the condensation of one mole of 2-pyridinecarbaldehyde with one mole of the corresponding aroylhydrazine in methanol.[8] Acetonitrile used for electrochemical and spectral studies was purified and dried according to a reported method.[24] All other chemicals and solvents used were of analytical grade available commercially and were used without further purification.

Physical measurements

Microanalytical (C, H, N) data were obtained with a Perkin-Elmer Model 240C elemental analyzer. A Shimadzu 3101-PC UV/vis/NIR spectrophotometer was used to record the electronic spectra. Infrared spectra were collected by using KBr pellets on a Jasco-5300 FT-IR spectrophotometer. ^{1}H NMR spectra of the complexes in $CDCl_3$ solutions were recorded on a Bruker 200 MHz spectrometer using $Si(CH_3)_4$ as an internal standard. Room temperature solid state magnetic susceptibilities were measured by using a Cahn magnetic susceptibility system consisting of a model 4600 adjustable gap electromagnet and a model 1000 electrobalance. Solution electrical conductivities were measured with a Digisun DI-909 conductivity meter. A CH-Instruments model 620A electrochemical analyzer was used for cyclic voltammetric and coulometric experiments with acetonitrile solutions of the complexes containing tetrabutylammonium perchlorate (TBAP) as supporting electrolyte. The three-electrode measurements were carried out at 298 K under a dinitrogen atmosphere with a glassy carbon working electrode, a platinum wire auxiliary electrode and an Ag–AgCl reference electrode. A platinum wire-gauze working electrode was used for coulometric experiments. Under identical condition the $E_{1/2}$ of the Fc^+/Fc couple was observed at +0.52 V (ΔE_p = 80 mV). The potentials reported in this work are uncorrected for junction contributions.

Synthesis of complexes

The complexes, $[Ru(pach)_2]$ (**1**), $[Ru(pabh)_2]$ (**2**), $[Ru(path)_2]$ (**3**), $[Ru(pamh)_2]$ (**4**), and $[Ru(padh)_2]$ (**5**), reported in this work were synthesized by the same general procedure in similar yields. Details are therefore given for a representative case.

$[Ru(pabh)_2]$ 2. To a yellow solution of Hpabh (101 mg, 0.45 mmol) and NaOH (18 mg, 0.45 mmol) in methanol (30 ml) was added solid $[Ru(dmso)_4Cl_2]$ (108 mg, 0.22 mmol). The mixture was refluxed for 12 h and then cooled to room temperature. The brown solid precipitated was collected by filtration, washed with ice-cold methanol and dried *in vacuum*. The purification of the complex was performed on a neutral aluminium oxide column. The first moving purple band was eluted with acetone–dichloromethane–hexane (1 : 5 : 5) mixture. This was collected and evaporated. The solid thus obtained was recrystallized from dichloromethane–hexane (1 : 1). Yield: 50 mg (41%).

Table 5 Crystal data and structure refinement for $[Ru(pabh)_2]$ **2**, $[Ru(path)_2]$ **3** and $[Ru(Hpabh)_2(CH_3CN)_2](ClO_4)_2 \cdot H_2O$ **6**

Complex	**2**	**3**	**6**
Chemical formula	$C_{26}H_{20}N_6O_2Ru$	$C_{28}H_{24}N_6O_2Ru$	$C_{30}H_{30}N_8O_{11}Cl_2Ru$
Formula weight	549.55	577.60	850.59
Space group	$P2_1/n$	$P2_1/n$	$P2_1/n$
a/Å	9.5802(14)	8.7422(17)	10.750(2)
b/Å	23.874(3)	8.6826(19)	27.396(5)
c/Å	10.3378(12)	33.738(5)	13.087(2)
β/°	105.102(13)	94.986(15)	95.054(16)
U/Å^3	2282.8(5)	2551.2(8)	3839.3(12)
Z	4	4	4
D_c/g cm^{-3}	1.599	1.504	1.472
μ/mm^{-1}	0.724	0.652	0.612
Reflections collected/unique	4133/4014	4822/4492	6875/6707
$R1$, $wR2$ [$I > 2\sigma(I)$]	0.0389, 0.0660	0.0518, 0.1079	0.0705, 0.1912
$R1$, $wR2$ (all data)	0.0716, 0.0754	0.1021, 0.1258	0.1176, 0.2231
Goodness-of-fit on F^2	1.03	1.047	1.025
Largest diff. peak and hole/e Å^{-3}	0.29 and −0.30	0.88 and −0.66	1.25 and −0.93

Spectrophotometric titration

In a typical titration, a 3 ml aliquot of a stock solution of $[Ru(pabh)_2]$ **2** in acetonitrile (3.66×10^{-5} M, prepared by dissolving 2.01 mg (3.66 μmol) of **2** in 10 ml of acetonitrile and then diluting 1 ml of this solution to 10 ml by adding the same solvent) was taken in an airtight cuvette. Protonation of **2** was performed by addition of aliquots (1 μL) of an acetonitrile solution of CF_3SO_3H (5.65×10^{-3} M, prepared by dissolving 0.5 ml (5.65 mmol) of CF_3SO_3H in 10 ml of acetonitrile and then diluting 0.1 ml of this solution to 10 ml by adding the same solvent) with a gastight syringe. Protonation was considered complete when no significant change of the electronic spectrum was observed by further addition of CF_3SO_3H solution.

X-Ray crystallography

Single crystals of $[Ru(pabh)_2]$ **2** and $[Ru(path)_2]$ **3** were grown by slow evaporation of CH_2Cl_2–hexane (1 : 1) solutions. Slow evaporation of a CH_3CN–toluene (1 : 1) solution of **2** and $HClO_4$ (1 : 2.5 mole ratio) in air at room temperature produced the single crystals of $[Ru(Hpabh)_2(CH_3CN)_2](ClO_4)_2 \cdot H_2O$ **6**. In each case, the crystal was mounted at the end of a glass fibre and covered with a thin layer of epoxy. The data were collected on an Enraf-Nonius Mach-3 single crystal diffractometer using graphite monochromated Mo Kα radiation ($\lambda = 0.71073$ Å) by the ω-scan method at room temperature (298 K). Unit cell parameters were determined by the least-squares fit of 25 machine-centred reflections. In each case, the stability of the crystal was monitored by measuring the intensities of three check reflections after every 1.5 h during the data collection. No decay was observed in any case. The data were corrected for Lorentz-polarization effects. An empirical absorption correction was applied on the data sets based on ψ-scans.[25] The structures were solved by direct methods and refined by full-matrix least-squares on F^2. All the three complexes crystallize in the $P2_1/n$ space group. In each case, the asymmetric unit contains a single molecule of the complex. For **3**, the tolyl ring (C22–C27, Fig. 2) of one of the ligands is disordered. The ring plane has two orientations. Three C-atoms (C22, C25 and C28) are common to both planes. Each of the other four C-atoms (C23, C24, C26 and C27) is found at two positions and refined with half occupancy. The oxygen of the water molecule in **6** was located at two sites and each was refined with half occupancy. For **2** and **3** all the non-hydrogen atoms and for **6** except the disordered water oxygen all other non-hydrogen atoms were refined anisotropically. Hydrogen atoms were added at calculated positions by using a riding model for structure factor calculation, but not refined. Calculations were done using the programs of WinGX[26] for data reduction and absorption correction, and SHELX-97 programs[27] for structure solution and refinement. The ORTEX6a package[28] was used for molecular graphics. Significant crystal data are summarized in Table 5.

CCDC reference numbers 175554–175556.

See http://www.rsc.org/suppdata/dt/b1/b110912j/ for crystallographic data in CIF or other electronic format.

Acknowledgements

Financial support by the Department of Science and Technology (DST), New Delhi (Grant No. SP/S1/F23/99) is gratefully acknowledged. Mr Satyanarayan Pal thanks the Council of Scientific and Industrial Research, New Delhi for a research fellowship. We thank Dr A. K. Bhuyan for helpful suggestions on analysis of the spectrophotometric titration data. X-Ray crystallographic studies were performed at the DST funded National Single Crystal Diffractometer Facility, School of Chemistry, University of Hyderabad.

References

1 E. A. Seddon and K. R. Seddon, *The Chemistry of Ruthenium*, Elsevier, Amsterdam, 1984; K. R. Seddon, *Coord. Chem. Rev.*, 1985, **67**, 171; A. Juris, V. Balzani, F. Barigelletti, S. Campagna, P. Belser and A. V. Zelewsky, *Coord. Chem. Rev.*, 1988, **84**, 85; B. K. Ghosh and A. Chakravorty, *Coord. Chem. Rev.*, 1989, **95**, 239; W. T. Wong, *Coord. Chem. Rev.*, 1994, **131**, 45; K. Kalyanasundaram, M. S. Lakeeruddin and M. K. Lakeeruddin, *Coord. Chem. Rev.*, 1994, **132**, 259; S. M. Lee and W. T. Wong, *Coord. Chem. Rev.*, 1997, **164**, 415; S. I. Gorelsky, E. S. Dodsworth, A. B. P. Lever and A. A. Vlcek, *Coord. Chem. Rev.*, 1998, **174**, 469.

2 M. Calvin, *J. Membrane Sci.*, 1987, **33**, 137; L. Sun, L. Hammarström, B. Åkermark and S. Styring, *Chem Soc. Rev.*, 2001, **30**, 36.

3 P. D. Beer, *Acc. Chem. Res.*, 1998, **31**, 71; J. P. Sauvage, J. P. Collin, J. C. Cambron, S. Guillerez, C. Coudret, V. Balzani, F. Barigelletti, L. De Cola and L. Flamingni, *Chem. Rev.*, 1994, **94**, 933; V. Balzani, A. Juris, M. Venturi, S. Campagna and S. Serroni, *Chem. Rev.*, 1996, **96**, 759.

4 H. B. Gray and J. R. Winkler, *Annu. Rev. Biochem.*, 1996, **65**, 537; J. K. Barton, in *Bioinorganic Chemistry*, ed. I. Bartini, H. B. Gray, S. J. Lippard and J. Valentine, University Science Books, Mill Valley, CA, 1994, p. 455; N. Sardesai, S. C. Lin, K. Zimmermann and J. K. Barton, *Bioconjugate Chem.*, 1995, **6**, 302; P. Lincoln, E. Tuite and B. Nordén, *J. Am. Chem. Soc.*, 1997, **119**, 1454.

5 S. Choudhury, A. K. Deb and S. Goswami, *J. Chem. Soc., Dalton Trans.*, 1994, 1305.

6 A. K. Das, S. M. Peng and S. Bhattacharya, *Polyhedron*, 2001, **20**, 327.

7 M. Ziegler, V. Monney, H. Stoeckli-Evans, A. V. Zelewsky, I. Sasaki, G. Dupic, J. C. Daran and G. G. A. Balavoine, *J. Chem. Soc., Dalton Trans.*, 1999, 667; J. E. Collins, J. J. S. Lamba, J. C. Love, J. E. McAlvin, C. Ng, B. P. Peters, X. Wu and C. L. Fraser, *Inorg. Chem.*, 1999, **38**, 2020; B. Geisser, A. Ponce and R. Alsfasser, *Inorg. Chem.*, 1999, **38**, 2030; A. Juris, L. Prodi, A. Harriman, R. Ziessel, M. Hissler, A. El-ghayoury, F. Wu, E. C. Riesgo and R. P. Thummel, *Inorg. Chem.*, 2000, **39**, 3590; X. Zhou, D. S. Tyson

and F. N. Castellano, *Angew. Chem., Int. Ed.*, 2000, **39**, 4301; L. H. Uppadine, M. G. B. Drew and P. D. Beer, *Chem. Commun.*, 2001, 291; H. Chao, G. Yang, G. Q. Xue, H. Li, H. Zang, I. D. Williams, L. N. Ji, X. M. Chen and X. Y. Li, *J. Chem. Soc., Dalton Trans.*, 2001, 1326.
8 N. R. Sangeetha, S. N. Pal and S. Pal, *Polyhedron*, 2000, **19**, 2713; S. N. Pal, K. R. Radhika and S. Pal, *Z. Anorg. Allg. Chem.*, 2001, **627**, 1631; N. R. Sangeetha, S. N. Pal, C. E. Anson, A. K. Powell and S. Pal, *Inorg. Chem. Commun.*, 2000, **3**, 415.
9 S. Baitalik, U. Flörke and K. Nag, *Inorg. Chem.*, 1999, **38**, 3296.
10 G. D. Storrier, S. B. Colbran and D. C. Craig, *J. Chem. Soc., Dalton Trans.*, 1997, 3011.
11 N. R. Sangeetha and S. Pal, *Polyhedron*, 2000, **19**, 1593; S. N. Pal, J. Pushparaju, N. R. Sangeetha and S. Pal, *Transition Met. Chem.*, 2000, **25**, 529.
12 R. M. Silverstein and F. X. Webster, in *Spectrometric Identification of Organic Compounds*, Wiley, New York, 6th edn., 1998, p. 101; K. Nakamoto, in *Infrared and Raman Spectra of Inorganic and Coordination Compounds*, Wiley, New York, 4th edn., 1986, p. 242.
13 S. N. Pal and S. Pal, *Inorg. Chem.*, 2001, **40**, 4807.
14 G. M. Brown, T. R. Weaver, F. R. Keene and T. J. Meyer, *Inorg. Chem.*, 1982, **21**, 3967.
15 J. March, in *Advanced Organic Chemistry*, Wiley, New York, 4th edn., 1998, p. 280.
16 D. P. Rillema, G. Allen, T. J. Meyer and D. Conrad, *Inorg. Chem.*, 1983, **22**, 1617.
17 C. M. Elliott and E. J. Hershenhart, *J. Am. Chem. Soc.*, 1982, **104**, 7519.
18 C. E. Dubé, D. W. Wright, S. Pal, P. J. Bonitatebus, Jr. and W. H. Armstrong, *J. Am. Chem. Soc.*, 1998, **120**, 3704.
19 K. Izutsu, in *Acid–Base Dissociation Constants in Dipolar Aprotic Solvents*, Blackwell, Oxford, 1990, p. 28.
20 D. D. Perrin, B. Dempsey and E. P. Serjeant, in *pK_a Prediction for Organic Acids and Bases*, Chapman and Hall, London and New York, 1981.
21 B. Mondal, S. Chakraborty, P. Munshi, M. G. Walawalkar and G. K. Lahiri, *J. Chem. Soc., Dalton Trans.*, 2000, 2327.
22 P. Braunstein, Y. Chauvin, J. Nahring, Y. Dusausoy, D. Bayeul, A. Tiripicchio and F. Ugozzoli, *J. Chem. Soc., Dalton Trans.*, 1995, 851.
23 I. P. Evans, A. Spencer and G. Wilkinson, *J. Chem. Soc., Dalton Trans.*, 1973, 204.
24 D. T. Sawyer and J. L. Roberts, Jr., in *Experimental Electrochemistry for Chemists*, Wiley, New York, 1974, p. 208.
25 A. C. T. North, D. C. Philips and F. S. Mathews, *Acta Crystallogr., Sect. A*, 1968, **24**, 351.
26 L. J. Farrugia, *J. Appl. Crystallogr.*, 1999, **32**, 837.
27 G. M. Sheldrick, SHELX-97 Structure Determination Software, University of Göttingen, Göttingen, Germany, 1997.
28 P. McArdle, *J. Appl. Crystallogr.*, 1995, **28**, 65.